NASA
Technical
Paper
2046

August 1982

Noise Transmission Loss of Aircraft Panels Using Acoustic Intensity Methods

Michael C. McGary

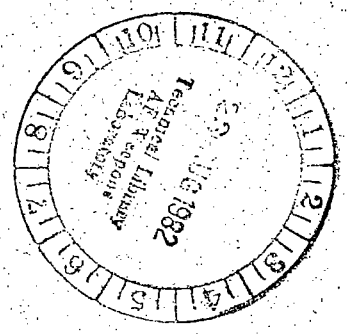

NASA

NASA
Technical
Paper
2046

1982

Noise Transmission Loss of Aircraft Panels Using Acoustic Intensity Methods

Michael C. McGary
Langley Research Center
Hampton, Virginia

National Aeronautics
and Space Administration

**Scientific and Technical
Information Branch**

SUMMARY

The two-microphone, cross-spectral technique for measuring acoustic intensity was used as a means for determining the acoustic transmission loss of aircraft panels. The study was aimed at interior noise of propeller-driven aircraft, so the measurements were restricted to the frequency regime below 1000 Hz. Two aircraft panel designs currently in use and one advanced design were studied. The effects of added damping were also studied for each of the three designs. The results indicate that the two-microphone, cross-spectral method for measuring acoustic intensity provides a reliable means of measuring net acoustic power flow through aircraft sidewalls. This method also has demonstrated advantages over the classical room acoustics method for measuring transmission loss.

INTRODUCTION

Interior noise levels of light propeller-driven aircraft have been measured between 84 and 104 dB on the A-weighted scale. (See ref. 1.) These noise levels are substantially higher than the levels for other types of aircraft with conventional take-off and landing and for ground transportation vehicles. Limited exposure to these noise levels can cause a temporary shift in the hearing threshold of the listener, and prolonged exposure could result in permanent hearing damage.

The distinguishing characteristic of interior noise for propeller-driven aircraft is the low-frequency tonal nature of the noise. The noise is caused primarily by the first few harmonics of the propeller blade-passage frequency and by the engine firing harmonics (if the aircraft is equipped with reciprocating engines). Maximum sound pressure levels typically occur in the frequency range from 80 to 200 Hz on the A-weighted scale. (See ref. 1.) This low-frequency character of the noise handicaps efforts to diagnose the path of the noise, and, because of weight considerations, renders many conventional noise control treatments impracticable.

Some information that is either necessary or desirable for designing an aircraft with quieter interior noise levels is as follows:

1. Transmission loss of the fuselage walls

2. Relative importance of structural and acoustic paths of the noise

3. Critical noise paths of the fuselage

4. Relative effectiveness of various add-on noise control treatments

Simple sound pressure level measurements are inadequate for producing this information. Near-field effects, multiple noise paths, source directivity, and reverberant effects all detract from the ability of the simple sound level meter to determine the source and path of the incoming noise. Attempts to identify noise paths in aircraft using the conventional lead wrapping technique have been unsuccessful because of the poor transmission loss of lead at low frequency. (See ref. 2.) This situation has forced the noise control engineer to search for faster, more economical methods of identifying and controlling aircraft interior noise.

Several new noise source/path identification tools have come into widespread use in recent years. Among the most promising of these new techniques are several methods for measuring the acoustic intensity vector. The two-microphone, cross-spectral method (refs. 3 through 5), the microphone-accelerometer cross-spectral method (refs. 6 through 10), and the near-field acoustic-holography method (refs. 11 through 13) have all been applied successfully to practical problems of interest for noise source/path identification purposes. The two-microphone method, in particular, has established itself as the standard measurement technique for problems of noise source/path identification in the automotive industry. In contrast, very little research or experimentation has been done to apply acoustic intensity measurement techniques to interior noise problems in aircraft.

Measurement of net acoustic power flow and transmission loss in narrow frequency bands is of critical importance in propeller-driven aircraft because of the discrete frequency character of propeller noise. If one of the propeller harmonics coincides with a structural resonance in the sidewall, very high interior noise levels can result. By using acoustic intensity techniques to measure transmission loss, the aircraft sidewall designer can locate the frequency bands in which the structural resonances occur and can determine the amount of noise that those resonances contribute. Appropriate measures can then be taken to shift or smooth the troublesome resonances through the use of add-on mass, stiffness, or damping treatments.

A second consideration in interior noise control of propeller-driven aircraft is added weight. Because these aircraft are sensitive to the addition of extra weight, the designer can add mass for noise control purposes only on the areas of the fuselage where it is absolutely necessary. The ability of acoustic intensity techniques to measure the net acoustic power flow or transmission loss as a function of position on the aircraft panel is then of paramount importance. With the information that acoustic intensity provides, the aircraft designer can minimize the weight penalty of add-on noise control treatments.

This paper is concerned primarily with the results of the noise transmission loss studies of six aircraft panel designs obtained by using the two-microphone, cross-spectral method of measuring acoustic intensity. The purpose of the study was twofold:

1. To gain further insight into the noise transmissive properties of aircraft panels

2. To determine the possible applications and uses of acoustic intensity methods as noise path identification tools for propeller-driven aircraft

SYMBOLS

A_w sum of surface area of walls in receiving room of transmission loss chamber

C_{xy} real part of cross spectrum (cospectrum)

c speed of sound in fluid medium

D/Dt substantial derivative or total derivative

e inverse natural logarithm of 1

f	frequency
G_{xx}	auto spectrum or power spectrum
G_{xy}	cross spectrum
g	acceleration due to gravity, $1g = 9.8\ m/sec^2$
$\vec{I}$	acoustic intensity vector
$\vec{I}_i$	incident acoustic intensity
$\vec{I}_t$	transmitted acoustic intensity
i	square root of -1
k	wave number
NR	noise reduction
P	Fourier transform of pressure
p	instantaneous pressure
p_{rms}	root-mean-square pressure
Q_{xy}	imaginary part of cross spectrum (quadrature spectrum)
R	room constant
Δr	spacing between microphones for acoustic intensity probe
SPL	sound pressure level
TL	transmission loss
TL_{FI}	field incidence transmission loss
t	time
V	Fourier transform of acoustic particle velocity
v	instantaneous acoustic particle velocity
X	Fourier transform of dummy variable x
x,y,z	dummy variables or Cartesian coordinates
θ	actual relative phase between microphones
λ	wavelength
μ	dynamic fluid viscosity
ρ	density of acoustic fluid medium

ϕ	measured relative phase between microphones
ψ	phase error introduced by instrumentation
ω	radial frequency
∇	gradient operator
∇^2	Laplacian operator
*	asterisk denotes complex conjugate
< >	triangular brackets denote an average over space or time

METHODS OF MEASURING ACOUSTIC TRANSMISSION LOSS

This study was conducted in the transmission loss apparatus in the Langley Aircraft Noise Reduction Laboratory. A transmission loss (TL) facility is traditionally used to measure the transmission loss of panels or other structural members. The conventional TL facility consists of two adjoining hard-walled reverberant chambers. The adjoining wall of the two chambers is made of thick, massive materials and is constructed so that the panel or structural member to be tested is mounted between the two rooms. This ensures that the primary acoustic path for sound travelling from one room into the adjoining room is through the panel being tested. One of the two adjoining rooms, designated the "source room," is where the sound source operates. The other room is designated the "receiving room," and is used to measure the sound transmitted through the panel.

Transmission loss is defined by the equation

$$TL = 10 \log_{10} \frac{\vec{I}_i}{\vec{I}_t} \tag{1}$$

where $\vec{I}_i$ is the incident intensity on the panel and $\vec{I}_t$ is the intensity transmitted through the panel.

Room Acoustics Method

The most widely used technique for measuring transmission loss with a TL facility is through the use of the classical room acoustics method. This method requires only two sound pressure level (SPL) measurements and a knowledge of the absorptive characteristics of the receiving room to implement transmission loss calculations. The difference between source-room and receiving-room sound pressure levels is called the noise reduction (NR) and is given as follows:

$$NR = SPL_{\text{source room}} - SPL_{\text{receiving room}} \tag{2}$$

Transmission loss is then calculated using the equation

$$TL = NR + 10 \log_{10} \frac{A_w}{R} \tag{3}$$

where A_w is the area of the walls in the receiving room and R is the room constant of the receiving room. References 14 through 16 provide more details on this measurement technique and on the relationship between equations (1) and (3).

When using the classical room acoustics method for measuring transmission loss, the requirements necessary for accurate measurement are as follows:

1. The reverberant fields in the source and receiving rooms are diffuse in the frequency range of interest. (See refs. 17 through 23 for more information regarding this essential requirement.)

2. The introduction of test panels must not significantly influence the acoustic absorptive characteristics of the receiving space.

3. The space averaged sound pressure level measurements must be performed at least one major source dimension away from the panel in the receiving room and at least one major source dimension away from the sound sources in the source room. (The measurements must be made under reverberant field conditions.)

Acoustic Intensity Method

Recent advances in multichannel digital signal processing have provided quick, reliable methods for measuring acoustic intensity. The time-averaged acoustic intensity-vector $\vec{I}$ is defined by

$$\vec{I} = \langle p\vec{v} \rangle_t \tag{4}$$

where p is the instantaneous sound pressure, $\vec{v}$ is the instantaneous particle velocity, and $\langle \rangle_t$ represents a time-averaged quantity. In the frequency domain, the magnitude of the acoustic intensity vector in the direction of the particle velocity is given by

$$\left|\vec{I}(f)\right| = \mathrm{Re}\left[P(f)\ V^*(f)\right] = C_{pv}(f) \tag{5}$$

where $P(f)$ is the complex Fourier transform of the pressure signal, $V^*(f)$ is the complex conjugate of the Fourier transform of the particle-velocity signal, and $C_{pv}(f)$ is the real part of the cross spectrum.

The acoustic intensity approach is attractive for three basic reasons:

1. It is based on the principles of conservation of energy and is therefore mathematically complete.

2. Intensity is a vector quantity and therefore provides directional information that sound pressure level measurements cannot.

3. It furnishes a method for determining the intrinsic acoustic transmissive and acoustic absorptive properties of materials.

The theory of the two-microphone, cross-spectral method of intensity measurement is well documented in the literature. (See refs. 3 to 5.) For the convenience of the reader, however, a derivation of the fundamental equations from the first principles is presented in appendix A. Additionally, a brief discussion of the most common sources of measurement error encountered when using the acoustic intensity method is presented in appendix B.

Application of the two-microphone, cross-spectral method to transmission loss measurements is simpler than the classical room acoustics method, and the requirements for the implementation of the measurements are less stringent. Recall the definition of transmission loss given by equation (1). The incident intensity $\vec{I}_i$ for the panel being tested may be calculated from the measured space-averaged sound pressure level in the source room. Assuming that the reverberant sound field in the source room is diffuse over the frequency range of interest, the relationship between the sound pressure and incident intensity is given by

$$|\vec{I}_i| = \frac{(p_{rms})^2}{4\rho c} \tag{6}$$

where ρc is the characteristic acoustic impedance, and p_{rms} is the space-averaged effective pressure in the source room. See reference 16 for a derivation of this equation. Equation (6) assumes that the sound impinging on the panel approaches at angles of incidence from 0° to 90° with equal probability (random incidence). A more realistic estimate of the intensity impinging on the panel is given by "field incident" intensity, which assumes angles of incidence from 0° to 78°. The corresponding equation for field incident intensity can be derived in the same manner as equation (6). The result is

$$|\vec{I}_i| = \frac{(p_{rms})^2}{4.18\rho c} \tag{7}$$

Once the space-averaged effective pressure in the source room is measured and the incident intensity is calculated, one needs only to measure the transmitted intensity using the two-microphone, cross-spectral method in order to complete the transmission loss calculations. The requirements for this measurement technique are as follows:

1. The reverberant acoustic field of the source room must be diffuse. (See refs. 17 through 23.)

2. The restrictions on the two-microphone intensity method as discussed in appendix B.

No restrictions are placed on the quality of the sound field or on the absorptive characteristics of the receiving room. This advantage over the classical room acoustics method has been verified experimentally. (See ref. 24.) Measurements have shown that neither reverberant nor anechoic conditions are necessary in the receiving space to obtain accurate results using this measurement technique. The two-microphone method has the added advantage of measuring transmission loss in narrow frequency bands (ref. 25), and is capable of localizing the noise transmission of a panel. (See refs. 24 and 25.)

EQUIPMENT AND PROCEDURES

Transmission Loss Apparatus

Figure 1 is a sketch of the transmission loss apparatus in the Langley Aircraft Noise Reduction Laboratory (ANRL) and the instrumentation used for the acoustic intensity measurements. Table I is a listing of some of the physical characteristics of the source room and receiving room of the transmission loss apparatus.

TABLE I.- PHYSICAL CHARACTERISTICS OF TRANSMISSION LOSS APPARATUS

	Dimensions, m	Surface area, m^2	Volume, m^3
Source room	3.73 × 2.90 × 3.89	73	42
Receiving room	2.74 × 2.90 × 4.06	62	32
Porthole between rooms	1.22 × 1.52	1.86	

These two hard-walled rooms do not meet the preferred minimum room volume (70 m^3) for precise determination of sound power levels of broad band noise at and below the 250-Hz, 1/3-octave frequency band. (See ref. 26.) Since the most troublesome noise sources on propeller-driven aircraft are the propeller harmonics in the 80-200 Hz frequency range, the relatively small volumes of the test chambers were of considerable concern during the planning stages of this research. As mentioned in the preceding section, the application of the two-microphone intensity method to transmission loss measurements requires a diffuse acoustic field in the source room. Consequently, a preliminary study aimed at quantifying the acoustic properties of the source and receiving rooms (ref. 23) was undertaken. The results of this study indicate that the acoustic diffusivity in the source room is adequate for transmission loss measurements over the 200-2000 Hz frequency range. Measurements of transmission loss below 200 Hz may be suspect because of the low acoustic modal density in the source room.

Another possible cause for concern is the effect of the reverberant field in the receiving room on the measurement accuracy of the two-microphone intensity method. It is generally agreed that the two-microphone method produces accurate results in direct and free-field situations. However, since the two-microphone probe measures the net intensity in a single direction, reverberation can have a detrimental effect on measurement accuracy. Results published in reference 24 suggest that any unfavorable effects due to reverberation can be negligible in practice, and at worst the errors introduced can be controlled by taking preventive measures. Consequently, as an added precaution, eight fiberglass panels were placed in the receiving room as shown in figure 1. These panels were 1.22 m × 2.44 m × 0.102 m. The fiberglass panels had the added benefit of reducing the ambient noise level in the receiving space.

Instrumentation

In the two-microphone cross-spectral method, intensity is calculated by using two closely spaced microphones near the noise source of interest. The microphone configuration is shown in figure 2. A dual-channel Fast Fourier analyzer processes the pressure signals from two microphones, and a computer is used to calculate intensity. Measurements of intensity are performed in practice by sweeping the hand-held two-microphone probe over the noise source while the Fast Fourier analyzer system gathers the data. This technique provides a space average and a time average simultaneously. A block diagram of the instrumentation is shown in figure 3.

The distance between the two microphones used for the acoustic intensity measurements is a function of the frequency range of interest. An aluminum bracket was constructed to hold two microphones (1.27 cm in diameter) apart at a fixed distance of 5 cm. This spacing was selected as the optimum microphone spacing for intensity measurements over the 100-1000 Hz frequency range. As an added precaution for signal conditioning, the microphone brackets were equipped with nylon sleeves to electrically isolate the microphone casings.

Test Panels

The noise transmission properties of six different aircraft panels were studied using the acoustic intensity measurement technique. A brief description of the physical characteristics of each of the six aircraft panels investigated follows:

Panel #1. The first panel tested was a skin-stiffened aluminum panel. A sketch of the panel as viewed from the receiving room is shown in figure 4. As shown in figure 4, this panel has an 0.81-mm thick aluminum skin with 4 vertical frame stiffeners and 10 horizontal stringers. The source of the design for the various components of the panel was a commercial general-aviation fuselage sidewall design.

Panel #2. A second skin-stiffened aluminum panel, built to the exact specifications as the first panel, was tested with the addition of a commercially available sound damping tape. The mass per unit area of the sound damping tape was 1.44 kg/m^2. This self-adhesive damping-tape material was added to the receiving-room side of the panel, completely covering the aluminum skin of the panel. The stringers and frames of the panel were left untreated (exposed). A total of 2.04 kg of damping-tape material was added to the panel, which amounts to a 29-percent increase in panel mass.

Panel #3. The third panel tested was a skin-stiffened aluminum panel with plexiglass windows. A sketch of the panel as viewed from the receiving room is shown in figure 5. The design of this panel is basically the same as the skin-stiffened aluminum panel. This panel, however, has three horizontal stringers that have been omitted and has three plexiglass windows that have been added. The mass per unit area of the plexiglass is 3.61 kg/m^2. The windows are 3.05 mm thick and are bolted in place on the panel. The windows are sealed with a 12.7-mm-wide, 0.8-mm-thick rubber gasket between the plexiglass and the aluminum skin.

Panel #4. A second skin-stiffened aluminum panel with windows (same specifications as the first windowed panel) was tested with the addition of sound damping tape. This self-adhesive damping-tape material was added to the

receiving-room side of the panel in a similar manner as before with the plain skin-stiffened aluminum panel. Only the windows, stringers, and frames of the panel were left untreated (exposed). Approximately 1.36 kg of damping-tape material was added to the panel which amounts to a 19-percent increase in panel mass.

Panel #5. A skin-stiffened aluminum panel modeled after an advanced turboprop sidewall design was also built and tested. A sketch of the panel as viewed from the receiving room is shown in figure 6. This panel has a 0.127-cm-thick aluminum skin with four vertical frame stiffeners and eight horizontal stringers. An analytical study of noise control by fuselage design techniques for advanced turboprop aircraft was the source of the panel design. (See ref. 27.)

Panel #6. A second advanced design panel (identical specifications) was built and tested with the addition of sound damping tape. The damping tape was added in a similar manner as with panels #2 and #4. Only the stringers and frames of the panel were left untreated. Approximately 2.04 kg of damping-tape material was added to the panel, which amounts to a 17-percent increase in panel mass.

A summary of the physical characteristics of the six aircraft panels tested is presented in table II. The exposed area in the source room of all panels is 1.69 m^2.

TABLE II.- PHYSICAL CHARACTERISTICS OF AIRCRAFT PANELS

Panel	Source of panel design	Plexiglass windows added	Damping tape added	Total panel mass, kg
#1	Current commercial general aviation panel design			6.82
#2			✓	8.86
#3		✓		7.27
#4		✓	✓	8.63
#5	Advanced turboprop design			12.05
#6			✓	14.09

Measurement and Analysis

The first step in the measurement procedure was the magnitude calibration of the microphones. A pistonphone provided a calibrated noise source of 124 dB at 250 Hz. Secondly, the two-microphone intensity probe was phase-calibrated using the apparatus shown in figure 7. The apparatus consists of a brass tube (2.54-cm inner diameter) with portholes at one end to flush mount two microphones. A white noise generator and acoustic driver provided a broadband noise source for the brass tube. The brass

tube was vibration-isolated from the driver using a flexible piece of plastic tubing as seen in figure 7. The apparatus produces accurate phase calibration information in the frequency range below the cut-on frequency of the acoustic cross modes in the brass tube (8000 Hz). The relative phase between the two microphones was measured and stored by the computer.

Once the microphones were calibrated, the two microphones used for the intensity measurements were placed in the bracket shown in figure 2, the microphone boom in the source room was turned on with a sweep rate of 16 seconds, and the speakers in the source room were turned on. (See fig. 1.) The microphone boom carriage was positioned in the center of the room at a height of 1.53 m. The boom swept a 2.5-m-diameter circle at an angle of 40° from horizontal. The closest approach of the boom to the boundaries of the room was 0.6 m, and the microphone was at no point closer than 1.2 m to either of the speakers in the source room.

The fast Fourier transform (FFT) analyzer-computer instrumentation system shown in figure 8 was used to digitize and record the sound pressure signal from the microphone boom in the source room. Four hundred ensemble averages (10 complete revolutions of the boom) were obtained by the FFT analyzer to ensure that a representative space-time average of the sound field in the source room was obtained. The sound pressure information was then stored by the computer. An example of the space-time-averaged sound pressure level spectrum in the source room is given in figure 9. A measurement of the source room SPL was performed each time a different panel was tested. The spectral characteristics of the sound field in the source room were identical for each of the six panels tested, and the overall SPL repeated to within 0.5 dB.

Once the source room SPL information was measured and stored, the acoustic intensity transmitted through the aircraft panel into the receiving room was measured using the two-microphone probe. Four hundred ensemble averages were completed for each space-time-averaged measurement of acoustic intensity. This ensured that the random portion of the statistical measurement error was less than 5 percent (assuming that the coherence between the two microphone signals is unity). The intensity probe was hand-held and slowly swept over a select portion of the aircraft panel with an approximately constant distance of 0.12 m between the center of the probe and the panel. Six intensity measurements were performed for each aircraft panel tested. The six areas of the panel that were separately analyzed are shown in figure 10. This particular arrangement of selected areas of analysis was dictated by the design of the panels. Two of the six panels tested had plexiglass windows in the areas designated in figure 10. The data were stored by the computer as cross spectra. The data were analyzed using the equations in appendix A in conjunction with equations (1) and (7). All phase and magnitude calibration factors were automatically included in the computer calculations.

MEASUREMENT RESULTS AND DISCUSSION

Transmission Loss Measurement Results

The results of the transmission loss measurements for the six panels are given in figures 11 through 16. Each figure represents narrow-band transmission loss data which was space-averaged over the entire area of the panel. The bandwidth in each of these six figures is 2.5 Hz. Each figure is plotted over the frequency range from 100-1000 Hz. Transmission loss data were available below 100 Hz, but were not considered accurate because the sound field in the source room is not diffuse at low

frequency. A summary of overall transmission loss levels, along with mass law comparisons for each of the six panels tested, is given in table III.

TABLE III.- OVERALL TRANSMISSION LOSS LEVELS FOR PANELS

Panel	TL_{FI}, dB, for -					
	100-1000 Hz		100-400 Hz		400-1000 Hz	
	Measured	Mass law	Measured	Mass law	Measured	Mass law
#1	17.5	15.3	12.9	11.5	18.0	20.7
#2	20.4	17.3	13.4	13.5	21.6	22.9
#3	18.7	15.8	13.7	12.0	19.3	21.2
#4	21.4	17.1	15.3	13.3	22.2	22.7
#5	20.7	19.8	13.7	15.9	22.1	25.5
#6	25.2	21.1	17.2	17.1	27.3	26.9

Figure 11 shows the transmission loss of the skin-stiffened aluminum panel (panel #1) over the 100-1000 Hz frequency range. The transmission loss curve of figure 11 shows four large structural resonances in the panel in the 100-200 Hz frequency range. (A structural resonance corresponds to a "dip" in the transmission loss curve.) The frequency ranges in which the first two structural resonances occur (122-128 Hz and 135-143 Hz) correspond to panel resonances measured at 121, 123, 126, 134.5, and 142 Hz using "tap tests" in a previous study of the panel dynamics. (See ref. 28.) Other resonances or combinations of resonant modes which radiate substantial amounts of noise occur in the 162-168 Hz and 200-205 Hz frequency ranges. The overall transmission loss of the panel in the 100-1000 Hz frequency range is 17.5 dB.

The dashed curve in figure 11 represents the mass law for this panel. This curve shows the transmission loss that a panel would produce if it had the same mass per unit area as panel #1 and was homogeneous, was infinite in extent (no boundary conditions), and had no stiffness or damping properties (pure mass). Mass law is the maximum transmission loss that a limp-mass, single-wall panel can attain. The nodal properties (caused by antiresonances) can sometimes cause the transmission loss behavior of a stiffened panel to exceed the mass law curve. (See fig. 11.)

The results of the transmission loss tests on the damped, stiffened aluminum panel (panel #2) are given in figure 12. The overall transmission loss of this panel in the 100-1000 Hz frequency range was 20.4 dB. This was a 2.9-dB increase in transmission loss compared with the first panel. Table III indicates that most of this increase occurs in the 400-1000 Hz frequency range. Calculations of the differences in overall transmission loss between the mass law curves in figures 11 and 12 (see table III) indicate that the increase in mass of the panel accounts for a 2.0-dB increase in overall transmission loss. The remaining increase in transmission loss can be attributed to damping effects and to the more isotropic distribution of panel mass. However, from the overall transmission loss levels given in table III and from the overall appearance of the two transmission loss curves, one can conclude that

the principal effect of the damping tape is that of an added mass. Any damping effects that exist tend to be small and are limited to the higher frequency ranges (600-1000 Hz).

Figure 13 shows the transmission loss of the skin-stiffened aluminum panel with windows (panel #3) measured over the 100-1000 Hz frequency range. The spectral characteristics of this figure are similar to the spectral characteristics of the transmission loss of the plain skin-stiffened aluminum panel (fig. 11). The structural resonances of the windowed panel below 400 Hz occur in exactly the same frequency regions as the resonances of the plain skin-stiffened aluminum panel. The overall transmission loss of the windowed panel in the 100-1000 Hz frequency range is 18.7 dB. This is a 1.2-dB greater transmission loss over the same frequency range than the panel without windows. This increase in the transmission loss may be partially attributed to the increased mass of the panel. The panel with windows is 7 percent heavier overall than the plain skin-stiffened aluminum panel. This relatively modest increase in panel mass, however, does not fully explain the 1.2-dB difference in transmission loss, because the difference in the mass law curves of figures 11 and 13 (see table III) accounts for only a 0.5-dB difference in overall transmission loss.

The results of the transmission loss measurements for the damped, windowed panel (panel #4) over the 100-1000 Hz frequency range are given in figure 14. Comparison of figure 14 with the transmission loss curve of the undamped, windowed panel (fig. 13) indicates that the effect of the damping tape is to increase and smooth the transmission loss curve in the 400-1000 Hz frequency range. The overall transmission loss in the 100-1000 Hz frequency range of the damped, windowed panel is 21.4 dB. This is a 2.7-dB increase in the transmission loss compared with the undamped case. The mass law curves of figures 13 and 14 (see table III) account for 1.3 dB of the difference in overall transmission loss. The remaining increase in transmission loss can be attributed primarily to the more isotropic mass distribution.

The results of the transmission loss tests for the advanced panel design (panel #5) are shown in figure 15. Structural resonances in the panel that are responsible for much of the noise transmission occur in the 120-128 Hz, 160-173 Hz, and 330-350 Hz frequency ranges. The overall transmission loss of the panel in the 100-1000 Hz frequency range is 20.7 dB. The overall appearance of the transmission loss curve is somewhat more "jagged" than the curves for the four panels discussed previously. The reasons for this apparent increase in the quality factor of the resonances is unclear.

The results of the transmission loss measurements for the damped, advanced panel design (panel #6) are given in figure 16. The overall transmission loss in the 100-1000 Hz frequency range of this panel was 25.2 dB. This is a 4.5-dB increase in transmission loss compared with panel #5. Table III indicates that much of this increase in transmission loss occurs in the 400-1000 Hz frequency range. Comparison of figure 16 with figure 15 indicates that the effect of the damping is to increase and smooth the transmission loss curve in the 300-1000 Hz frequency range. The increased damping effects (the smoothing of the transmission loss curve) is more pronounced and occurs over a much larger frequency range (300-1000 Hz) than was measured for panels #2 and #4. These panels showed possible increased damping only in the 600-1000 Hz frequency range. The difference in the mass law curves of figures 15 and 16 (see table III) account for 1.3 dB of the difference in overall transmission loss. Hence, most of the increase in transmission loss can be attributed to the increased damping effects and to the more isotropic mass distribution of the damped, advanced design panel (panel #6).

Comparison of Localized Acoustic Intensity Measurements

The space-averaged acoustic intensity transmitted through the entire skin-stiffened aluminum panel (panel #1) is shown in figure 17. This curve is representative of the spectral-intensity plots obtained from the six different areas of the panel. Figure 18 is a comparison of the overall acoustic intensity over the 2.5-1000 Hz frequency range transmitted through each of the six areas of the panel. (See fig. 10 for a sketch of the six areas.) Figure 18 shows that the measured acoustic intensity transmitted through the six areas differed at most by 0.9 dB.

The overall acoustic intensities transmitted through the six different measurement areas of the skin-stiffened aluminum panel with windows (panel #3) are shown in figure 19. The lower half of the panel (areas 4, 5, and 6) transmits about the same amount of noise as the upper half of the panel (areas 1, 2, and 3). This result is expected since the mass per unit area of the aluminum skin (0.214 g/cm^2) is not significantly different from the mass per unit area of the plexiglass windows (0.361 g/cm^2).

The overall acoustic intensities transmitted through the six different areas of the damped, windowed panel (panel #4) are shown in figure 20. It is evident that the upper portion of the panel (areas 1, 2, and 3) transmits more noise than the lower half of the panel (areas 4, 5, and 6).

A comparison of the overall acoustic intensities (2.5-1000 Hz) transmitted through the lower and upper halves of the damped and undamped windowed panels (panels #3 and #4) is shown in figure 21. This figure shows that once the damping tape has been added to the panel, further add-on treatments of mass or damping to the skin of the panel may be ineffective, because the windows have become the principal contributer of the transmitted noise.

CONCLUDING REMARKS

Several conclusions can be drawn about the aircraft panels tested. The measurement results indicate that the noise transmissive properties of all panels tested could be improved initially if they had a more isotropic mass distribution. The addition of damping materials could also be beneficial to all panel designs. The add-on damping treatment appeared to be particularly effective in reducing the noise transmission of the advanced design panel (panel #5). In general, the effectiveness of damping treatment depends on the frequency range and the quality (severeness) of the resonant noise transmission. The damping treatment is most effective for the high-frequency range (above 600 Hz).

The results also indicate that the addition of plexiglass windows improved the noise transmission loss of the plain stiffened aluminum panel. This improvement was slight, however, and was probably caused by the added mass of the windows. The tests also show that when damping and extra mass are added to the windowed panels, the windows rapidly become the principal noise elements of the panel. This fact can be important when designing an interior trim panel for an aircraft sidewall. The designer must be careful not to direct his noise control efforts solely at the metallic portions of the panel.

The noise transmissive properties measured in this paper are probably not representative of the actual transmission loss of similar panels under flight conditions. This is because of the significant differences in the noise sources and the boundary

conditions on the panel. The effects of the boundary conditions are most important in the low-frequency regime. Therefore, the structural resonances observed in the panels tested would probably be "shifted" to different frequency regimes on similar panels tested in flight.

The results of the study indicate that the two-microphone, cross-spectral method of acoustic intensity measurement is a powerful noise source/path identification tool. This method provides a quick, reliable means of measuring net acoustic power flow through aircraft sidewalls, and has demonstrated advantages over the classical room acoustics method for measuring transmission loss. The three principal advantages of the intensity method are:

1. Measurement of transmission loss in narrow frequency bands

2. Measurement of transmission loss as a function of position on the test panel

3. No special requirements are placed on the acoustic qualities of the receiving space.

The ability of the acoustic-intensity measurement technique to measure net acoustic power flow independent of the acoustic qualities of the receiving space will become more important as time progresses and new studies are performed. Since the interior of an aircraft cabin is neither an anechoic nor a reverberant receiving space, the acoustic-intensity method holds considerable promise for determining the noise transmissive properties of aircraft sidewalls under flight conditions.

Langley Research Center
National Aeronautics and Space Administration
Hampton, VA 23665
July 2, 1982

APPENDIX A

THEORY OF TWO-MICROPHONE, CROSS-SPECTRAL METHOD OF ACOUSTIC INTENSITY MEASUREMENT

The Navier-Stokes equation of momentum conservation for incompressible, constant-viscosity flow is given by

$$\rho \frac{D\vec{v}}{Dt} = \rho\vec{g} - \nabla p + \mu\nabla^2\vec{v} \tag{A1}$$

where ρ is the density of the fluid medium, μ is the coefficient of dynamic viscosity, ∇ is the gradient operator, ∇^2 is the Laplacian, $\vec{g}$ is the acceleration due to gravity, and D/Dt is the substantial derivative given by

$$\frac{D}{Dt} = \frac{\partial}{\partial t} + \vec{v}_x \frac{\partial}{\partial x} + \vec{v}_y \frac{\partial}{\partial y} + \vec{v}_z \frac{\partial}{\partial z} \tag{A2}$$

If the effects of gravity and viscosity are neglected, equation (A1) becomes

$$\frac{D\vec{v}}{Dt} = -\frac{1}{\rho}\nabla p \tag{A3}$$

Making a small perturbation assumption (neglecting higher order terms) changes equation (A3) to

$$\frac{\partial\vec{v}}{\partial t} = -\frac{1}{\rho}\nabla p \tag{A4}$$

If the analysis is confined to a single dimension, equation (A4) becomes

$$\frac{\partial\vec{v}_x}{\partial t} = -\frac{1}{\rho}\frac{\partial p}{\partial x} \tag{A5}$$

Making a finite-difference approximation for the pressure gradient yields

$$\frac{\partial\vec{v}_x}{\partial t} = -\frac{1}{\rho\,\Delta r}(p_2 - p_1) \tag{A6}$$

where Δr is the spacing between two microphones. If the Fourier transform is defined as

$$X(\omega) = \int_{-\infty}^{\infty} x(t)e^{-i\omega t}\,dt \tag{A7}$$

and this transform is applied to equation (A6), then

$$\int_{-\infty}^{\infty} \frac{\partial \vec{v}_x}{\partial t} e^{-i\omega t}\, dt = -\frac{1}{\rho\, \Delta r}\left[P_2(\omega) - P_1(\omega)\right] \tag{A8}$$

Integrating the left side of equation (A8) by parts yields

$$i\omega \int_{-\infty}^{\infty} \vec{v}_x e^{-i\omega t}\, dt = -\frac{1}{\rho\, \Delta r}\left[P_2(\omega) - P_1(\omega)\right] \tag{A9}$$

If these terms are rearranged, then

$$\int_{-\infty}^{\infty} \vec{v}_x e^{-i\omega t}\, dt = \frac{i}{\rho\omega\, \Delta r}\left[P_2(\omega) - P_1(\omega)\right] \tag{A10}$$

The term on the left side of equation (A10) is the Fourier transform of the particle velocity. Therefore,

$$V(\omega) = \frac{i}{\rho\omega\, \Delta r}\left[P_2(\omega) - P_1(\omega)\right] \tag{A11}$$

Equation (A11) is an approximation of the particle velocity at a point midway between two microphones. The pressure midway between two microphones can be estimated by

$$P(\omega) = \frac{P_2(\omega) + P_1(\omega)}{2} \tag{A12}$$

Substituting into equation (5) then yields

$$\begin{aligned} \left|\vec{I}(\omega)\right| &= \mathrm{Re}\left[P(\omega)\, V^*(\omega)\right] \\ &= \mathrm{Re}\left[\frac{i}{2\rho\omega\, \Delta r}\left(P_1P_1^* - P_2P_2^* + P_2P_1^* - P_2^*P_1\right)\right] \end{aligned} \tag{A13}$$

The terms inside the parentheses are recognized as the auto spectra and cross spectra between microphone signals 1 and 2. (See ref. 29 for details.) The definitions for auto spectra and cross spectra are as follows:

$$G_{xx} = P_x^*P_x \tag{A14}$$

$$G_{xy} = C_{xy} - iQ_{xy} = P_x^*P_y \tag{A15}$$

These definitions can be used to write equation (A13) as follows:

$$|\vec{I}(\omega)| = \mathrm{Re}\left[\frac{i}{2\rho\omega\,\Delta r}(G_{11} - G_{22} - 2iQ_{12})\right] \tag{A16}$$

If the real part of the right side of equation (A16) is taken as indicated, the result is

$$|\vec{I}(\omega)| = \frac{Q_{12}}{\rho\omega\,\Delta r} \tag{A17}$$

where Q_{12} is the imaginary part of the cross spectrum between microphones 1 and 2 (the quadrature spectrum).

APPENDIX B

SOURCES OF ERROR ASSOCIATED WITH ACOUSTIC INTENSITY MEASUREMENT TECHNIQUE

There are four principal sources of error associated with the two-microphone, cross-spectral method. They are as follows:

1. Instrumentation phase mismatch

2. Finite-difference error

3. Directional effects and errors of interpretation

4. Near-field effects

For the convenience of the reader, a brief discussion of each type of error is presented here. More detailed discussions are contained in references 30 through 32.

The cross spectrum G_{xy} (eq. (A15)) was defined by the conjugate multiplication of the complex Fourier transforms $P_x(\omega)$ and $P_y(\omega)$. These complex Fourier transforms may be expressed in complex polar form as follows:

$$P_x(\omega) = |P_x(\omega)| \exp[i\phi_x(\omega)] \tag{B1}$$

Equation (A15) can then be written as

$$G_{xy} = |P_x| \; |P_y| \exp[i(\phi_x - \phi_y)] \tag{B2}$$

and equation (A17) can be rewritten as

$$|\vec{I}(\omega)| = \frac{|P_1| \; |P_2| \sin(\phi_1 - \phi_2)}{\rho\omega \; \Delta r} \tag{B3}$$

It is obvious from equation (B3) that the magnitude of the intensity vector is proportional to the sine of the relative phase difference between the two microphones. The relative phase difference $(\phi_1 - \phi_2$ or $\Delta\phi)$ has two components and may be written as follows:

$$\Delta\phi = \Delta\theta_{physics} + \Delta\psi_{instruments} \tag{B4}$$

where ϕ is the measured relative phase, $\theta_{physics}$ is the actual relative phase, and $\psi_{instruments}$ is the relative phase error introduced by the instrumentation phase mismatch. This error occurs primarily in the low-frequency regime. Elimination of instrumentation phase mismatch may be approached in one of two ways. One method proposed by Chung et al. (ref. 5) uses a microphone interchange technique to

eliminate this type of error. The more common method is to carefully measure the instrumentation phase mismatch and compensate for it in subsequent computer calculations.

The second type of error introduced by the two-microphone method is the error associated with the finite-difference approximation of equation (A6). This error occurs primarily in the high-frequency regime. To assure that this error is small, it should be required that

$$k\,\Delta r = \frac{\omega}{c}\,\Delta r = \frac{2\pi\,\Delta r}{\lambda} << \frac{\pi}{2} \tag{B5}$$

or

$$\frac{\Delta r}{\lambda} << \frac{1}{4} \tag{B6}$$

where Δr is the spacing between microphones, and λ is the wavelength of interest.

The third type of measurement error stems from misinterpretation of results. Directional effects and multiple sources can result in the measurement of components of intensity vectors unintended by the measurer. Careful planning and excecution of the measurements can help to prevent the acquisition of data contaminated with acoustic intensity vector components from unwanted sound sources. Reference 30 contains a computer study of this type of error.

The fourth, and probably least experienced, type of error is near-field measurement error. In theory, the large pressure gradients in the near field of higher order acoustic sources such as dipoles and quadrapoles can cause considerable error in the measurement accuracy of the two-microphone method. For a detailed discussion of this type of error, see reference 31.

REFERENCES

1. Catherines, John J.; and Mayes, William H.: Interior Noise Levels of Two Propeller-Driven Light Aircraft. NASA TM X-72716, 1975.

2. Jha, S. K.; and Catherines, J. J.: Interior Noise Studies for General Aviation Types of Aircraft, Part II: Laboratory Studies. J. Sound & Vib., vol. 58, no. 3, June 8, 1978, pp. 391-406.

3. Fahy, Frank J.: Measurement of Acoustic Intensity Using the Cross-Spectral Density of Two Microphone Signals. J. Acoust. Soc. America, vol. 62, no. 4, Oct. 1977, pp. 1057-1059.

4. Lambrich, H. P.; and Stahel, W. A.: A Sound Intensity Meter and Its Applications in Car Acoustics. INTER-NOISE 77 Proceedings - Noise Control: The Engineer's Responsibility, Eric J. Rathe, ed., c.1977, pp. B 142 - B 147.

5. Chung, J. Y.; Pope, J.; and Feldmaier, D. A.: Application of Acoustic Intensity Measurement to Engine Noise Evaluation. Diesel Engine Noise Conference, Proc. P-80, Soc. Automot. Eng., c.1979, pp. 353-364. (Available as SAE [preprint] 790502.)

6. Czarnecki, Stefan; Engel, Zbigniw; and Panuszka, Ryszard: Correlation Method of Measurements of Sound Power in the Near-Field Conditions. Arch. Acoust., vol. 1, no. 3, 1976, pp. 201-213.

7. Hodgson, Thomas H.: Investigation of the Surface Acoustical Intensity Method for Determining the Noise Sound Power of a Large Machine In Situ. J. Acoust. Soc. America, vol. 61, no. 2, Feb. 1977, pp. 487-493.

8. Brito, J. Daniel: Machinery Noise Source Analysis Using Surface Intensity Measurements. NOISE-CON 79 Proceedings - Machinery Noise Control, Joseph W. Sullivan and Malcolm J. Crocker, eds., c.1979, pp. 137-142.

9. McGary, Michael C.: Noise Source Identification of Diesel Engines Using Surface Intensity Measurement. M.S. Thesis, Purdue Univ., 1980.

10. Boone, Diane E.; and Hodgson, Thomas H.: Surface Intensity Measurements Using a Fiber Optic-Pressure Probe. Recent Developments in Acoustic Intensity Measurement, Cent. Tech. Ind. Mec., c.1981, pp. 89-94.

11. Williams, Earl G.; and Maynard, Julian D.: Intensity Vector Field Mapping With Nearfield Holography. Recent Developments in Acoustic Intensity Measurement, Cent. Tech. Ind. Mec., c.1981, pp. 31-36.

12. Williams, Earl G.; Maynard, J. D.; and Skudrzyk, Eugen: Sound Source Reconstructions Using a Microphone Array. J. Acoust. Soc. America, vol. 68, no. 1, July 1980, pp. 340-344.

13. Maynard, J. D.; and Williams, E. G.: Nearfield Holography, a New Technique for Noise Radiation Measurement. NOISE-CON 81 Proceedings - Applied Noise Control Technology, Larry H. Royster, Franklin D. Hart, and Noral D. Stewart, eds., c.1981, pp. 19-24.

14. Lyon, R. H.; Dietrich, C. W.; Ungar, E. E.; Pyle, R. W., Jr.; and Apfel, R. E.: Low-Frequency Noise Reduction of Spacecraft Structures. NASA CR-589, 1966.

15. Ver, Istvan L.; and Holmer, Curtis I.: Interaction of Sound Waves With Solid Structures. Noise and Vibration Control, Leo L. Beranek, ed., McGraw-Hill Book Co., c.1971, pp. 270-361.

16. Kinsler, Lawrence E.; and Frey, Austin R.: Fundamentals of Acoustics, Second ed. John Wiley & Sons, Inc., c.1962.

17. Cook, Richard K.; Waterhouse, R. V.; Berendt, R. D.; Edelman, Seymour; and Thompson, M. C., Jr.: Measurement of Correlation Coefficients in Reverberant Sound Fields. J. Acoust. Soc. America, vol. 27, no. 6, Nov. 1955, pp. 1072-1077.

18. Doak, P. E.: Fluctuations of the Sound Pressure Level in Rooms When the Receiver Position Is Varied. Acustica, vol. 9, no. 1, 1959, pp. 1-9.

19. Schroeder, Manfred R.: Measurement of Sound Diffusion in Reverberation Chambers. J. Acoust. Soc. America, vol. 31, no. 11, Nov. 1959, pp. 1407-1414.

20. Morrow, Charles T.: Point-to-Point Correlation of Sound Pressures in Reverberation Chambers. Shock & Vib. Bull., Bull. 39, Pt. 2, U.S. Dep. Def., Feb. 1969, pp. 87-97.

21. De Bruijn, A.: Influence of Diffusivity on the Transmission Loss of a Single-Leaf Wall. J. Acoust. Soc. America, vol. 47, no. 3, pt. 1, Mar. 1970, pp. 667-675.

22. Chu, W. T.: Comments on the Coherent and Incoherent Nature of a Reverberant Sound Field. J. Acoust. Soc. America, vol. 69, no. 6, June 1981, pp. 1710-1715.

23. McGary, Michael C.: Sound Field Diffusivity in NASA Langley Research Center Hardwalled Acoustic Facilities. NASA TM-83275, 1982.

24. Crocker, Malcolm J.; Forssen, Bjorn; Raju, P. K.; and Mielnicka, Anna: Measurement of Transmission Loss of Panels by an Acoustic Intensity Technique. INTER-NOISE 80 Proceedings - Noise Control for the 80's, Volume II, George C. Maling, Jr., ed., c.1980, pp. 741-746.

25. McGary, Michael C.: Interior Noise Source/Path Identification on Propeller-Driven Aircraft Using Acoustic Intensity Methods. NOISE-CON 81 Proceedings - Applied Noise Control Technology, Larry H. Royster, Franklin D. Hart, and Noral D. Stewart, eds., c.1981, pp. 261-264.

26. Precision Methods for the Determination of Sound Power Levels of Broad-Band Noise Sources in Reverberation Rooms. ANSI S1.31-1980 (ASA 11-1980), Acoust. Soc. America, c.1980.

27. Revell, J. D.; Balena, F. J.; and Koval, L. R.: Analytical Study of Interior Noise Control by Fuselage Design Techniques on High-Speed, Propeller-Driven Aircraft. NASA CR-159222, 1978.

28. Mixson, J. S.; Roussos, L. A.; Barton, C. K.; Vaicaitis, R.; and Slazak, M.: Laboratory Study of Efficient Add-On Treatments for Interior Noise Control in Light Aircraft. AIAA-81-1969, Oct. 1981.

29. Bendat, Julius S.; and Piersol, Allan G.: Random Data: Analysis and Measurement Procedures. John Wiley & Sons, Inc., c.1971.

30. Lyon, Richard H.: DD6. Some Observations on Sound Intensity Measurements. Program of the 99th Meeting. J. Acoust. Soc. America, vol. 67, suppl. 1, Spring 1980, p. S70.

31. Thompson, J. K.; and Tree, D. R.: Finite Difference Approximation Errors in Acoustic Intensity Measurements. J. Sound & Vib., vol. 75, no. 2, Mar. 22, 1981, pp. 229-238.

32. Seybert, A. F.: Statistical Errors in Acoustic Intensity Measurements. J. Sound & Vib., vol. 75, no. 4, Apr. 22, 1981, pp. 519-526.

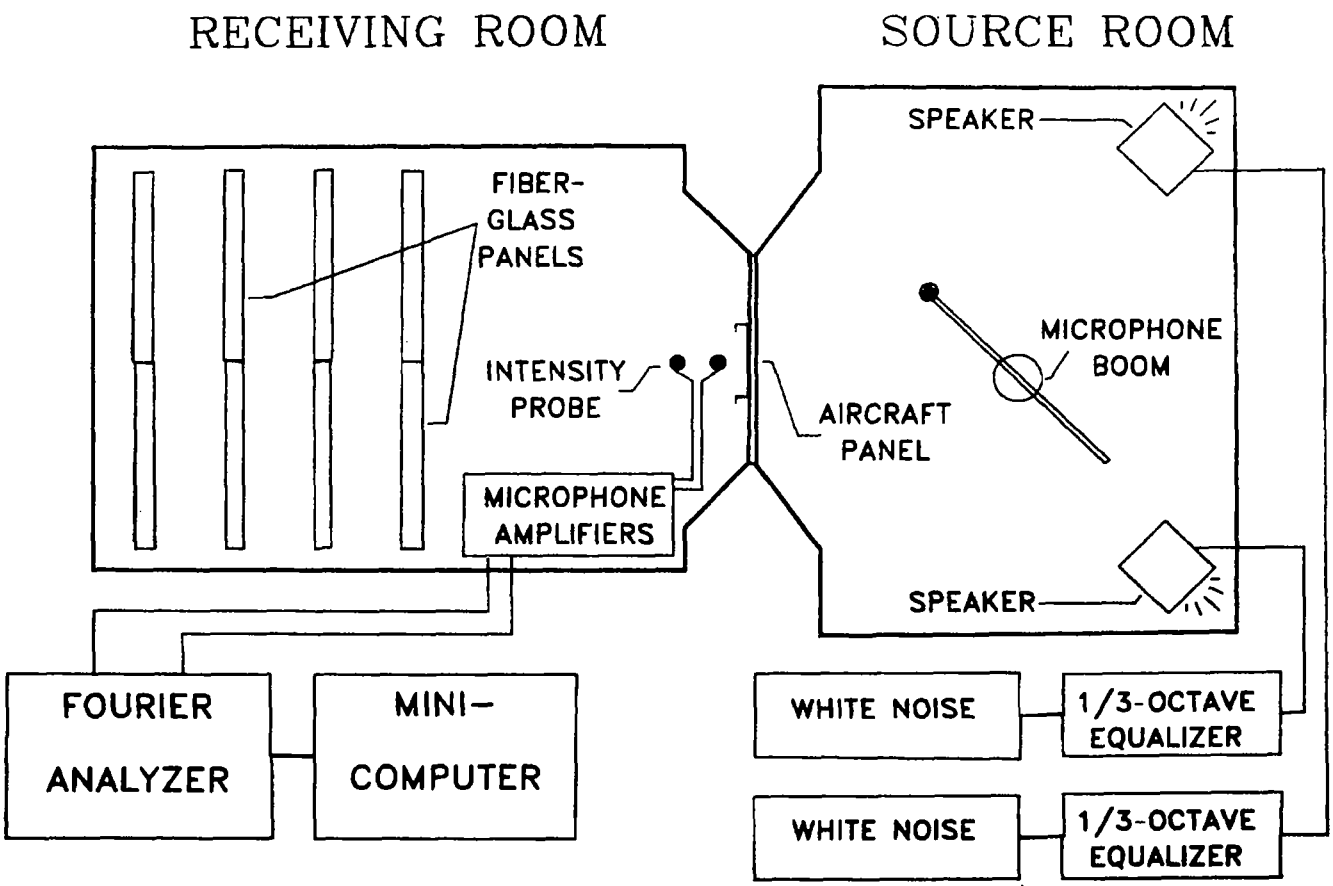

Figure 1.- Sketch of ANRL transmission loss apparatus.

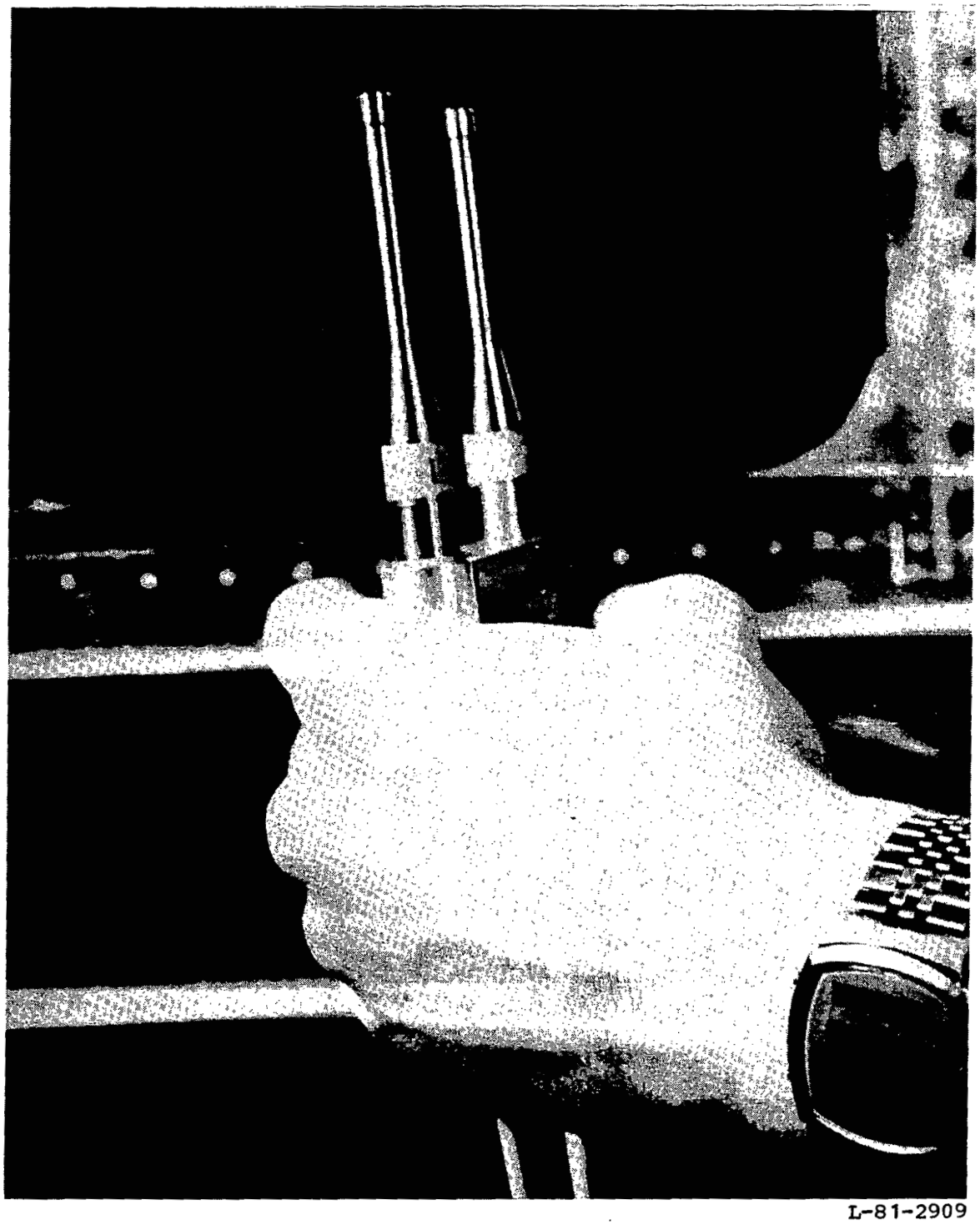

L-81-2909

Figure 2.- Intensity probe.

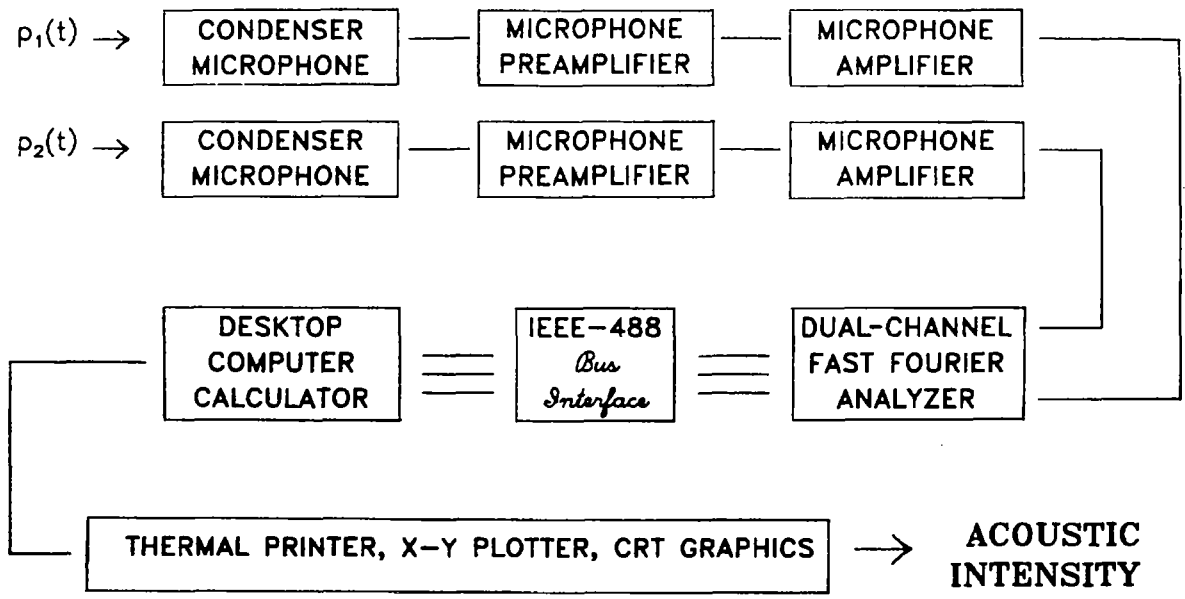

Figure 3.- Receiving-room instrumentation.

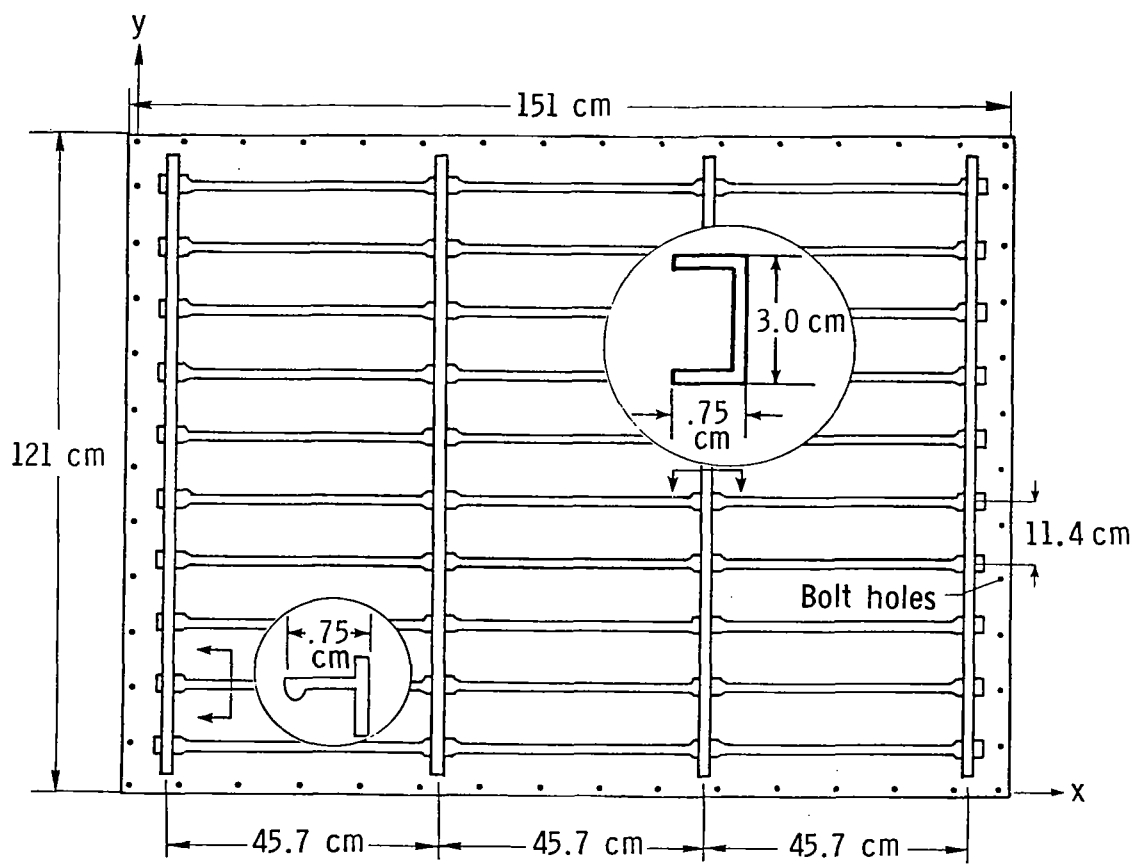

Figure 4.- Skin-stiffened aluminum test panel (panel #1). Aluminum skin is 0.0813 cm thick.

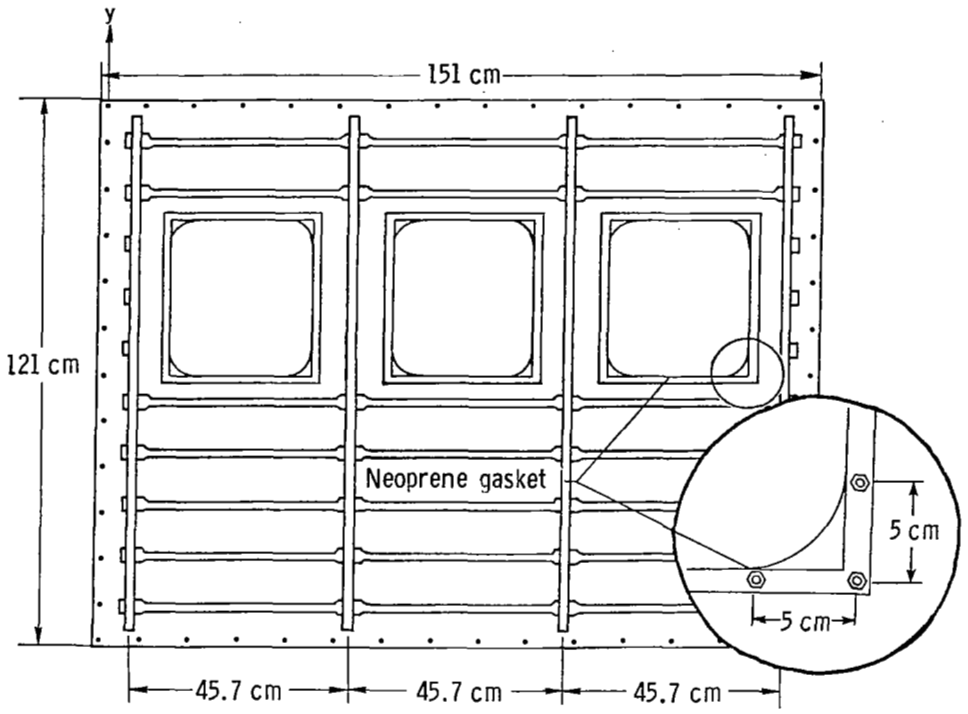

Figure 5.- Stiffened test panel with windows (panel #3). Aluminum skin is 0.0813 cm thick; plexiglass windows are 0.305 cm thick.

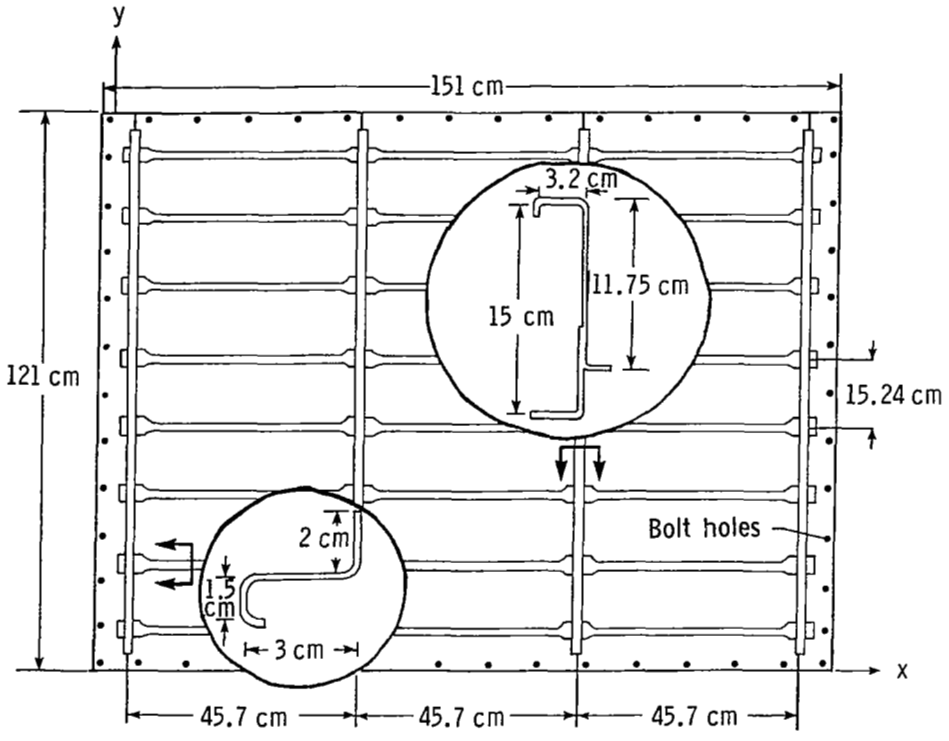

Figure 6.- Advanced design panel (panel #5). Aluminum skin is 0.127 cm thick.

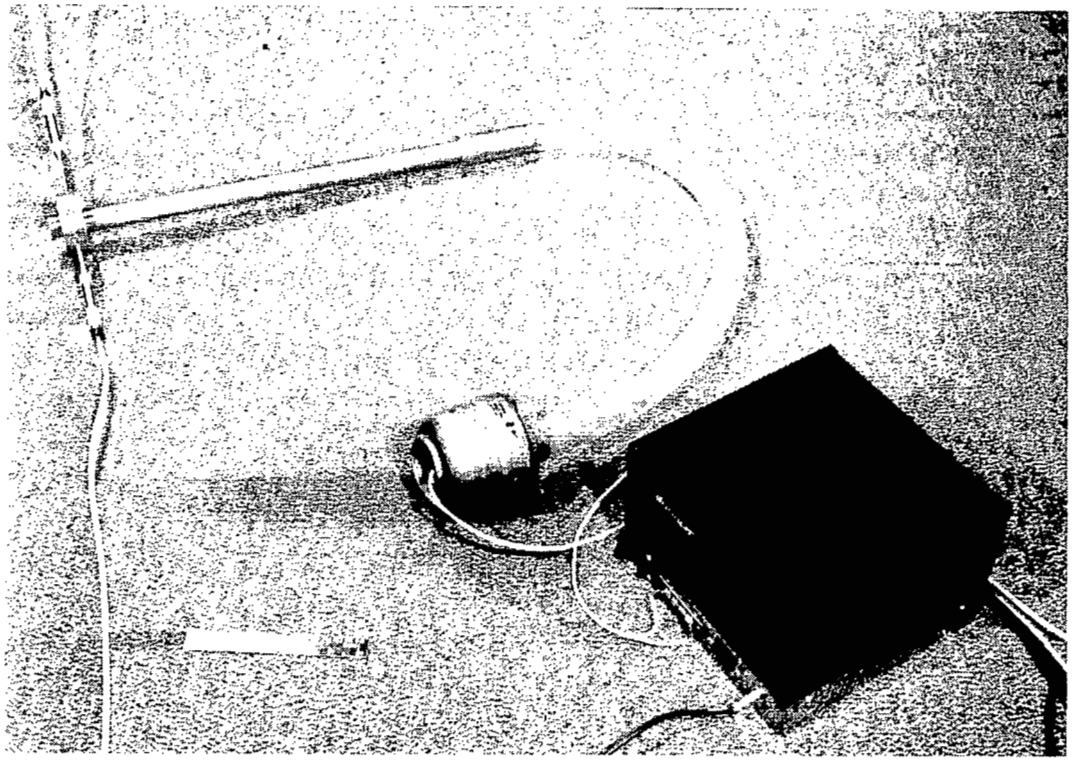

L-81-2916

Figure 7.- Phase calibration device.

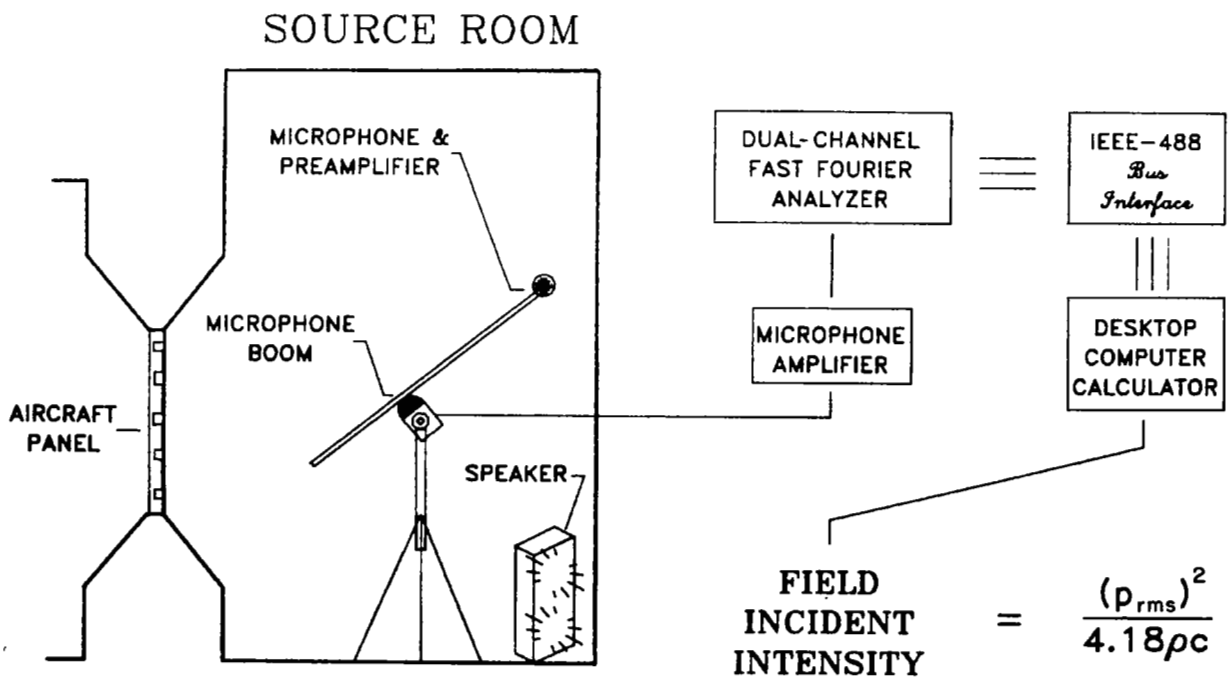

Figure 8.- Source-room instrumentation.

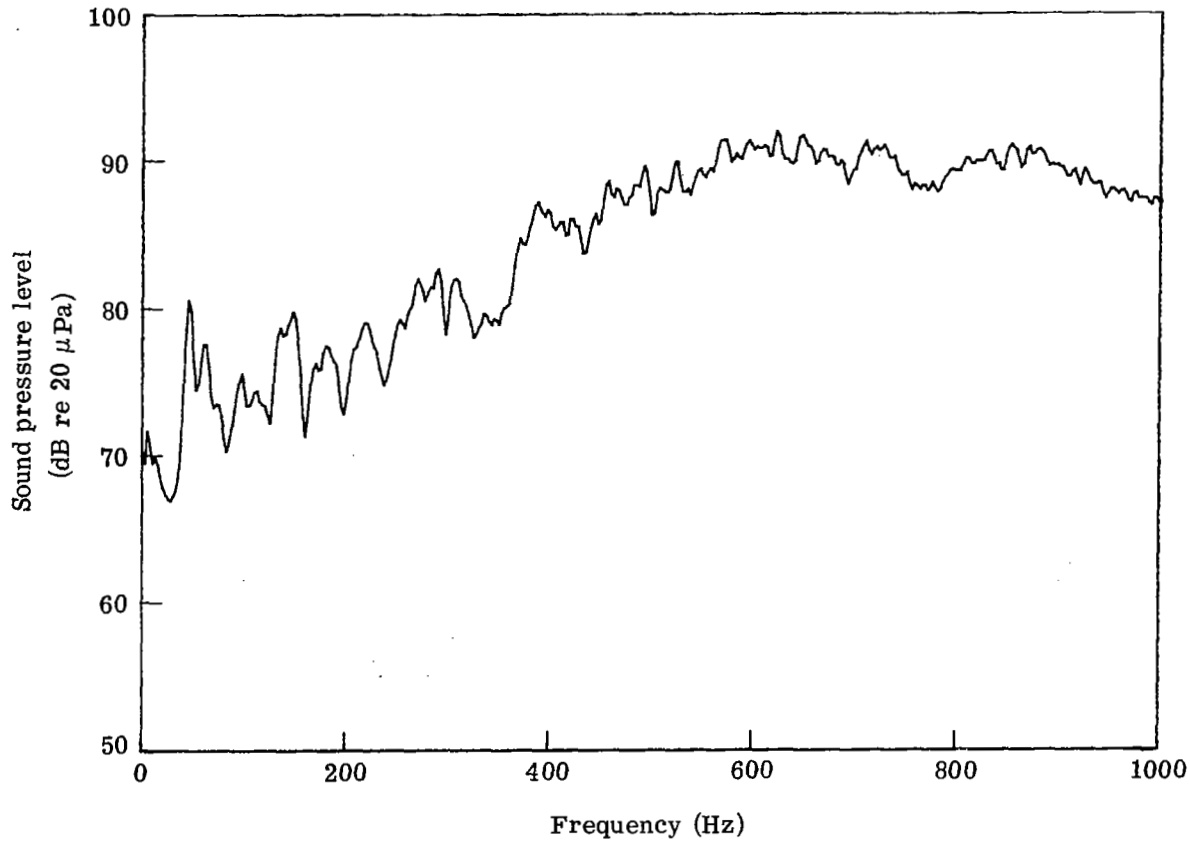

Figure 9.- Typical sound pressure level in source room.

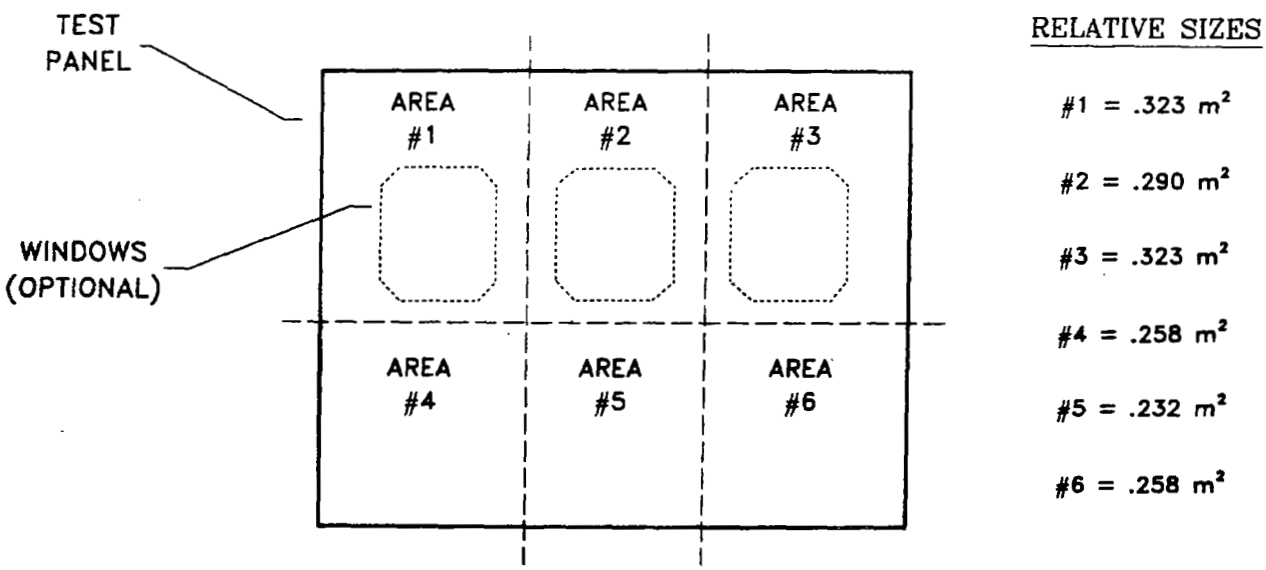

Figure 10.- Selected panel areas.

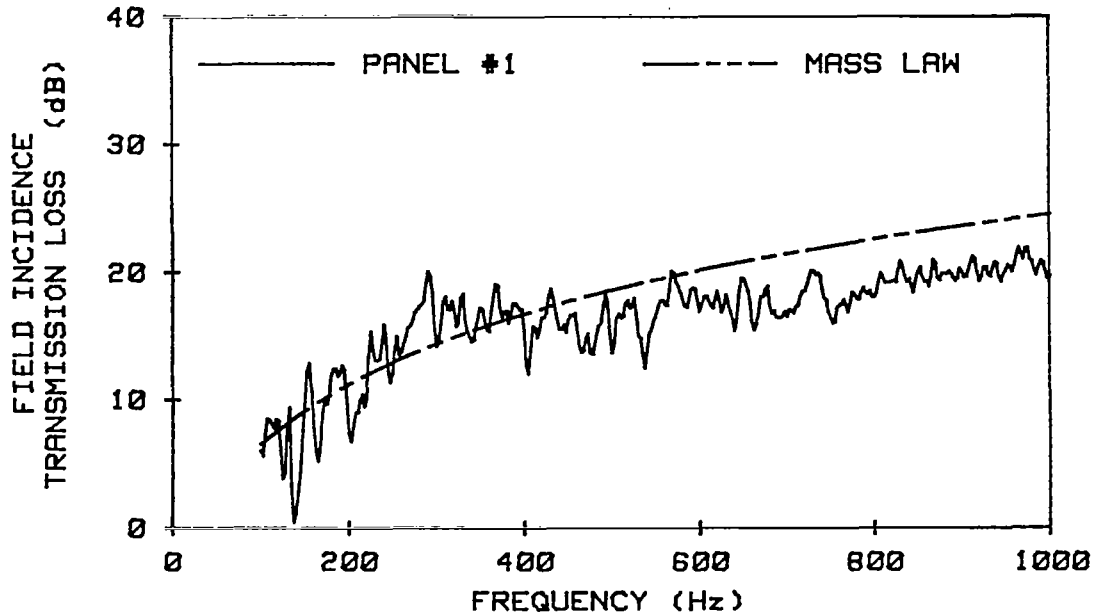

Figure 11.- Transmission loss of skin-stiffened aluminum panel (panel #1).

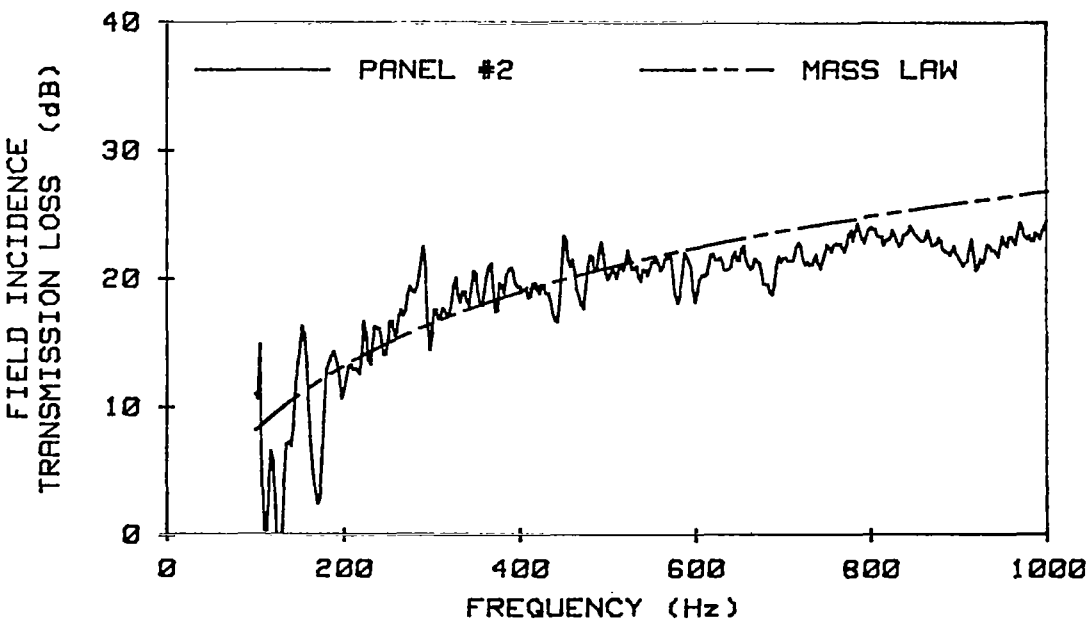

Figure 12.- Transmission loss of skin-stiffened panel with added damping (panel #2).

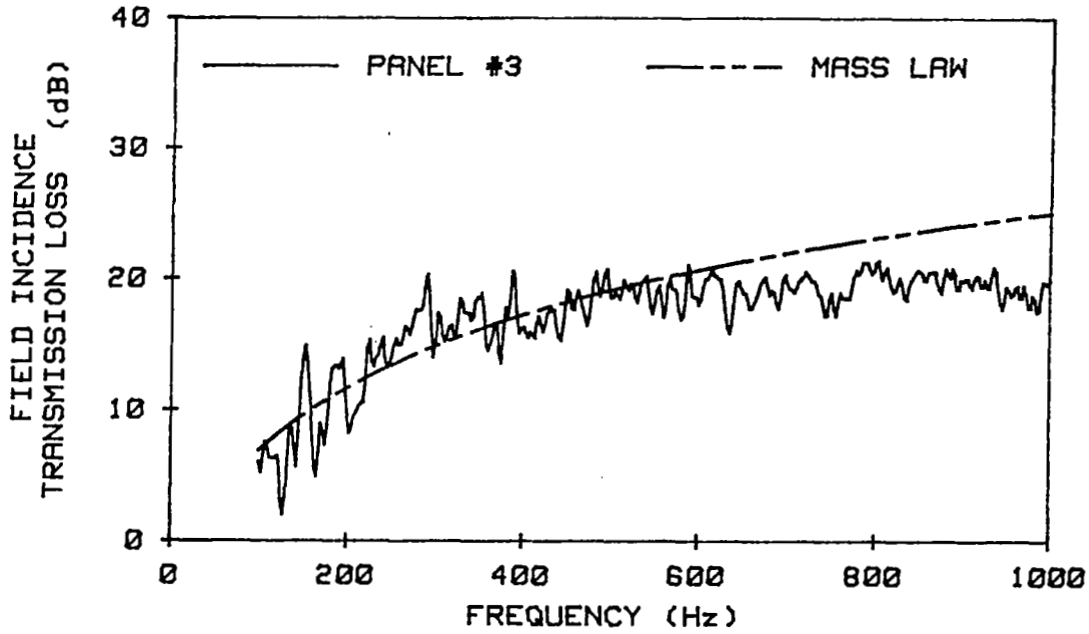

Figure 13.- Transmission loss of skin-stiffened aluminum panel with windows (panel #3).

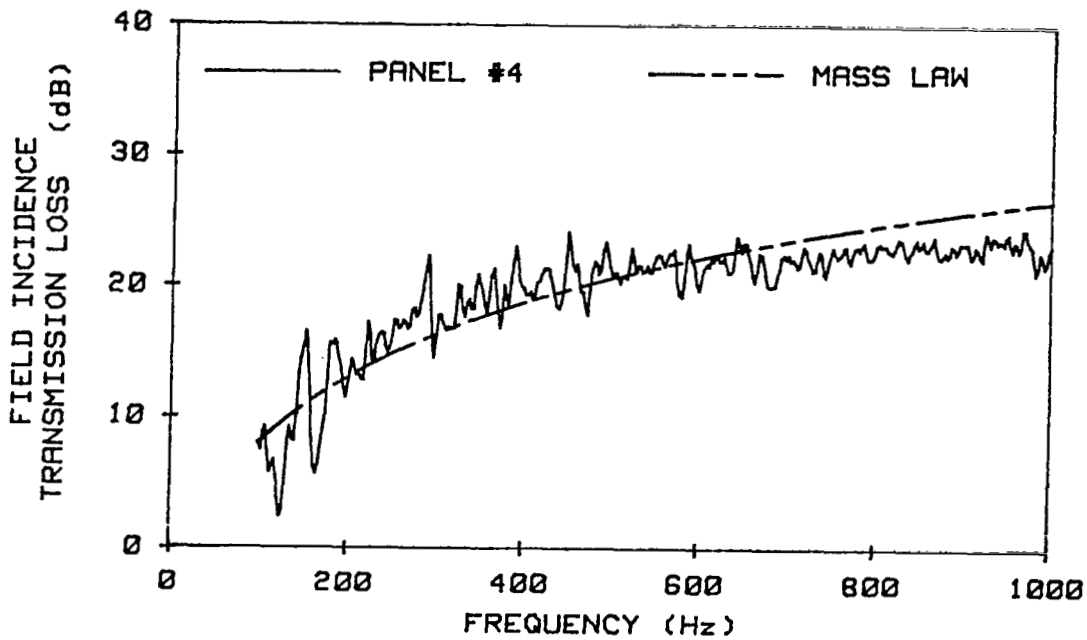

Figure 14.- Transmission loss of skin-stiffened panel with windows and damping (panel #4).

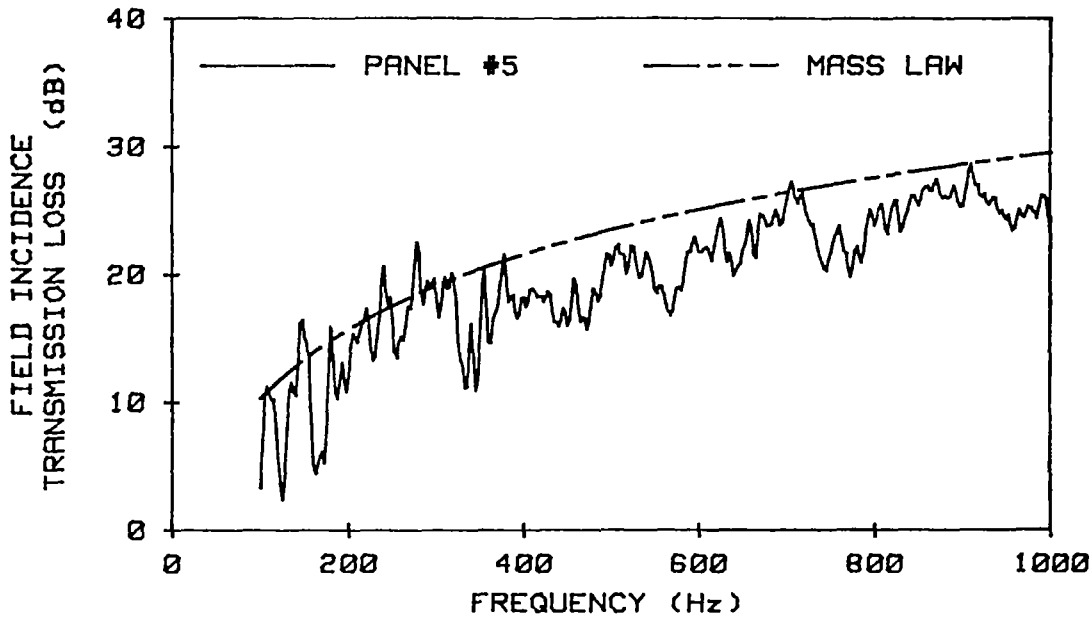

Figure 15.- Transmission loss of advanced design panel (panel #5).

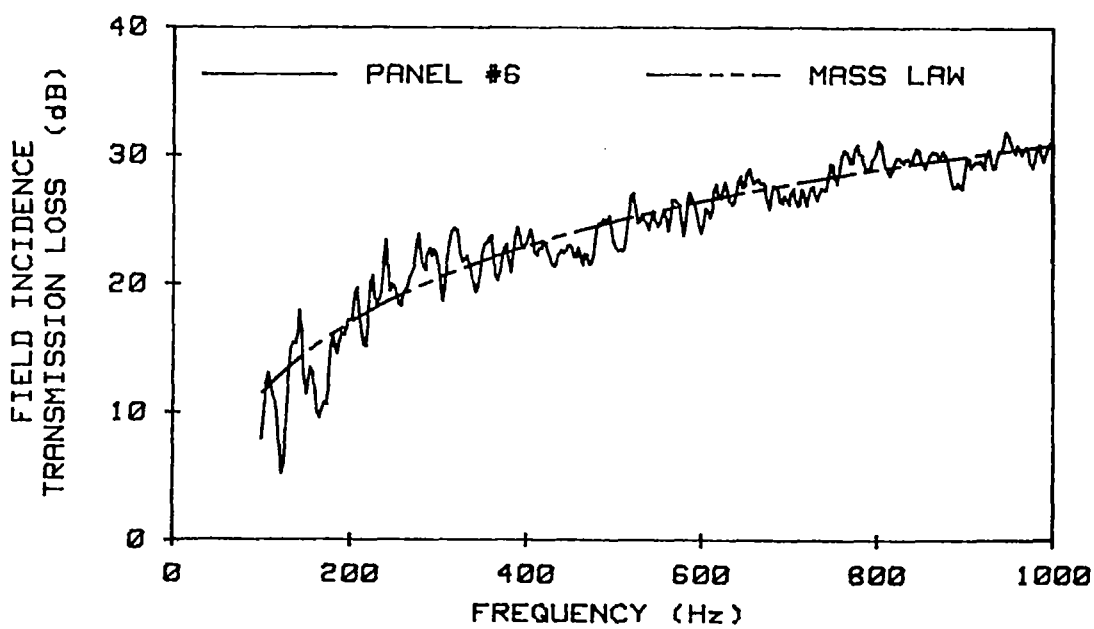

Figure 16.- Transmission loss of advanced design panel with added damping (panel #6).

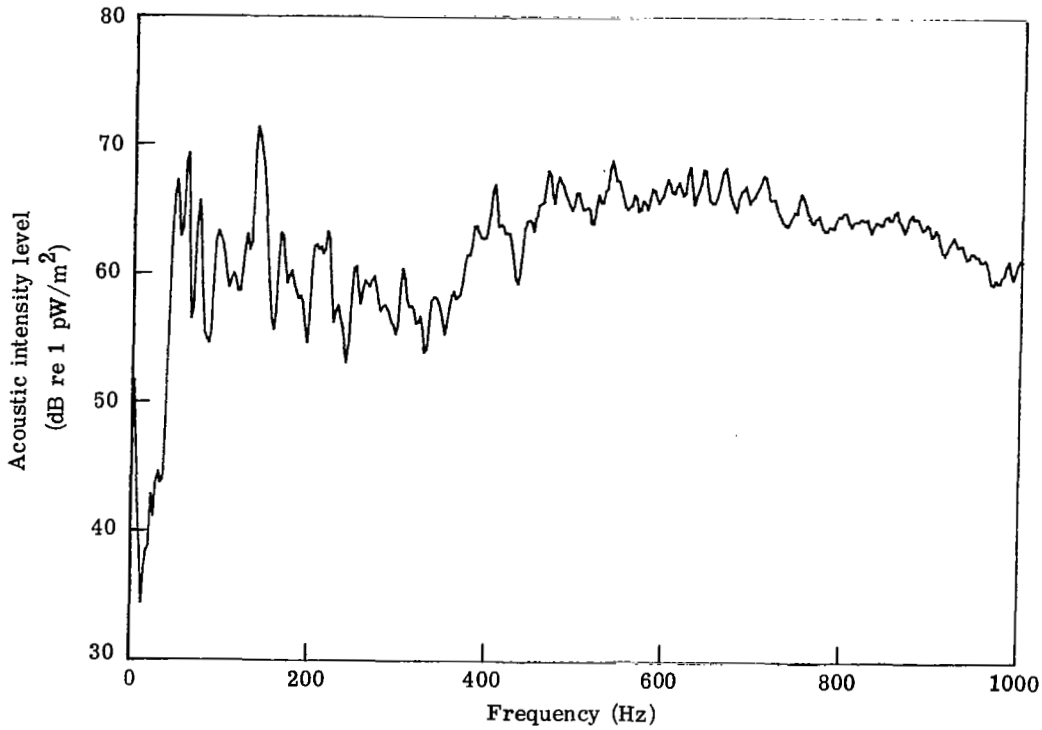

Figure 17.- Space-averaged acoustic intensity transmitted through panel #1.

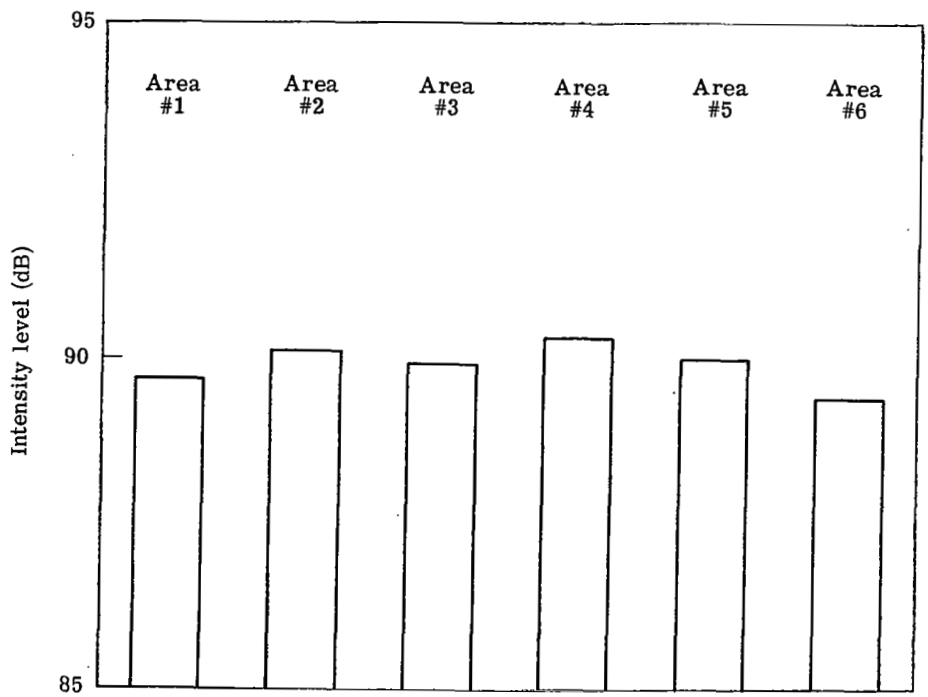

Figure 18.- Noise transmitted through various parts of skin-stiffened aluminum panel (panel #1) for 2.5-1000 Hz.

Figure 19.- Noise transmitted through various parts of windowed panel (panel #3) for 2.5-1000 Hz.

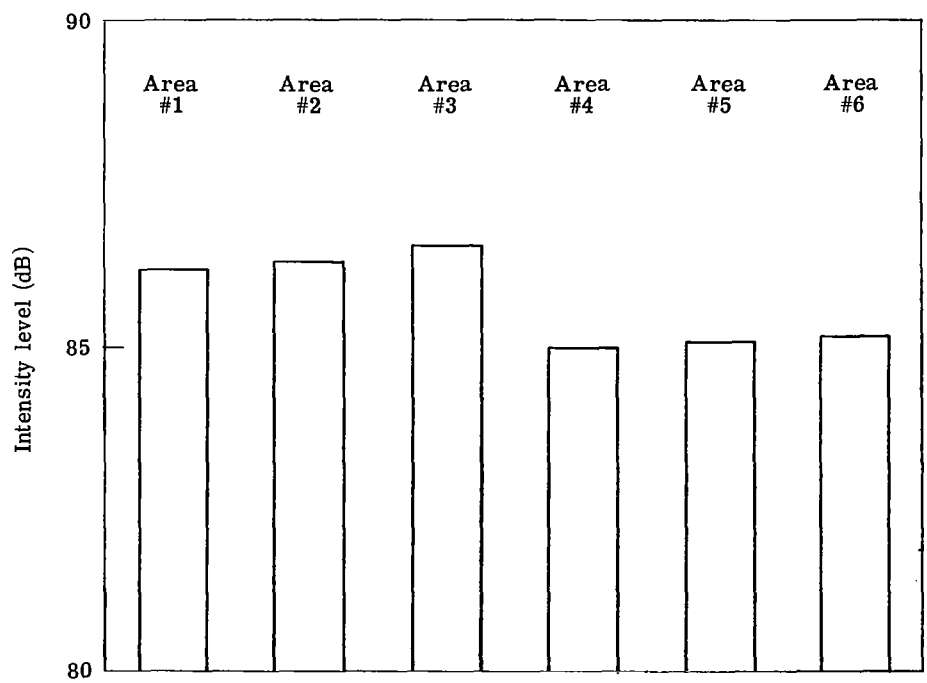

Figure 20.- Noise transmitted through various parts of damped, windowed panel (panel #4) for 2.5-1000 Hz.

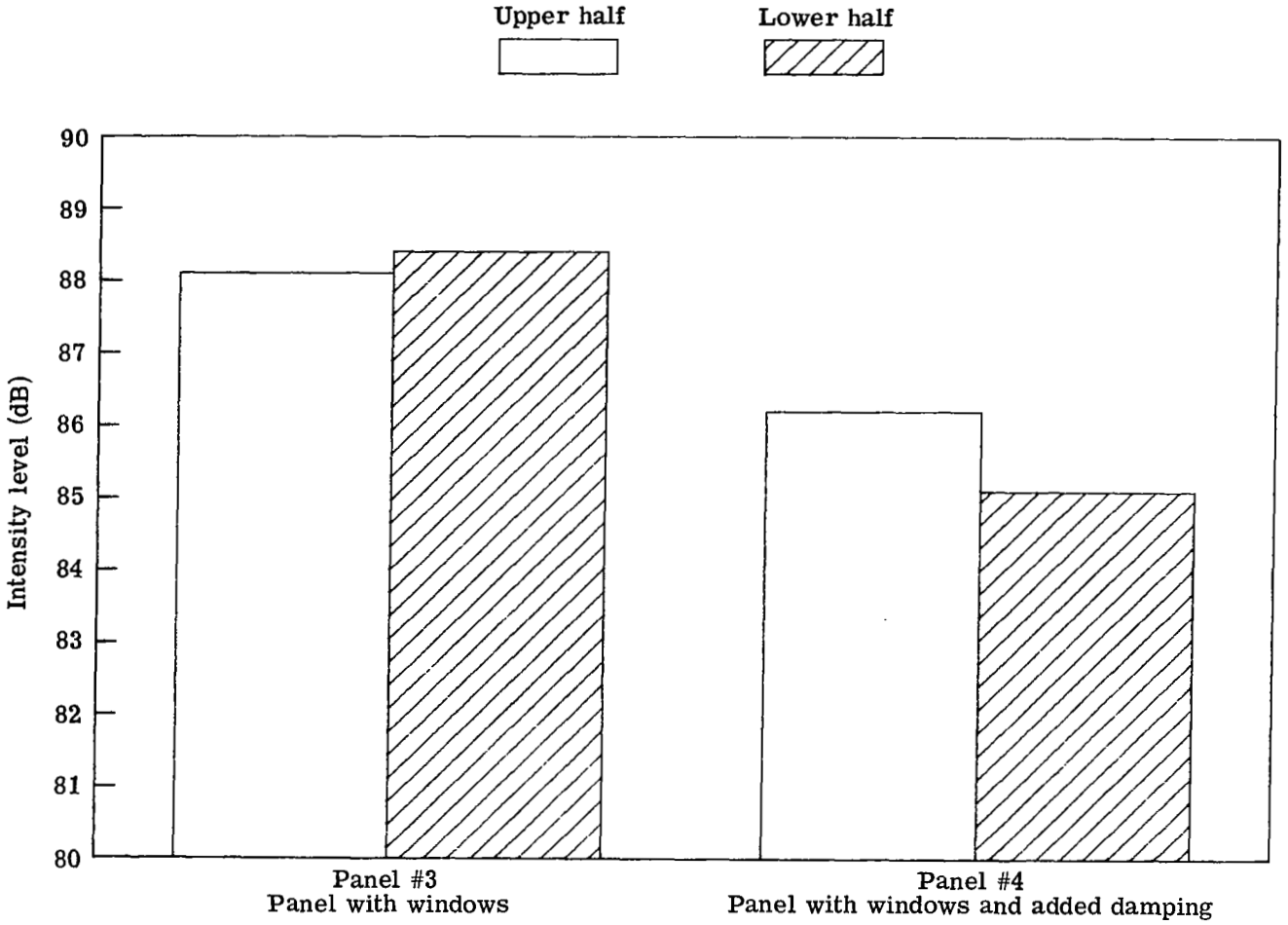

Figure 21.- Comparison of transmitted noise for panels with windows for 2.5-1000 Hz.

1. Report No.	2. Government Accession No.	3. Recipient's Catalog No.
NASA TP-2046		

4. Title and Subtitle	5. Report Date
NOISE TRANSMISSION LOSS OF AIRCRAFT PANELS USING ACOUSTIC INTENSITY METHODS	August 1982
	6. Performing Organization Code 505-33-53-03
7. Author(s) Michael C. McGary	8. Performing Organization Report No. L-15306
	10. Work Unit No.
9. Performing Organization Name and Address NASA Langley Research Center Hampton, VA 23665	11. Contract or Grant No.
	13. Type of Report and Period Covered Technical Paper
12. Sponsoring Agency Name and Address National Aeronautics and Space Administration Washington, DC 20546	14. Sponsoring Agency Code

15. Supplementary Notes

16. Abstract

The two-microphone, cross-spectral, acoustic intensity measurement technique was used to determine the acoustic transmission loss of three different aircraft panels. The study was conducted in the transmission loss apparatus in the Langley Aircraft Noise Reduction Laboratory.

17. Key Words (Suggested by Author(s))	18. Distribution Statement
Acoustic intensity Transmission loss Aircraft interior noise Noise source identification Noise path identification Propeller noise	Unclassified - Unlimited Subject Category 71

19. Security Classif. (of this report)	20. Security Classif. (of this page)	21. No. of Pages	22. Price
Unclassified	Unclassified	35	A03

For sale by the National Technical Information Service, Springfield, Virginia 22161

NASA-Langley, 1982